



23rd International Conference on Knowledge-Based and Intelligent Information & Engineering Systems

## In Underground Vehicular Radio Channel Characterization

Hamou Chehri<sup>a</sup>, Abdellah Chehri<sup>b\*</sup>, Nadir Hakem<sup>c</sup>

<sup>a</sup> Bell-Canada, 671 Rue de la Gauchetière Ouest, Montréal, Québec, H3B 2M8, Canada.

<sup>b</sup> Department of Applied Sciences, University of Quebec in Chicoutimi (UQAC), Chicoutimi, G7H 2B1, Québec, Canada.

<sup>c</sup> University of Quebec in Abitibi-Témiscamingue (UQAT), Val-d'Or, J9P 6W6, Québec, Canada.

---

### Abstract

Vehicular communication is characterized by a dynamic environment and high mobility. In this paper we present a shadow fading model targeting system simulations based on real measurements performed in underground gallery. As first results, we present in this paper the delay spread statistics for each investigated environment. We also study the large-scale, small-scale fading and extract some time channel parameters such as root-mean-square (RMS) delay for a realistic underground propagation environment at 5.9 GHz. Since there are so far few published results for these confined environments, the results obtained can be useful for the deployment of vehicular-to-vehicular (V2V) and vehicular-to-infrastructure (V2I) communication systems inside underground mines galleries.

© 2019 The Authors. Published by Elsevier B.V.

This is an open access article under the CC BY-NC-ND license (<https://creativecommons.org/licenses/by-nc-nd/4.0/>)  
Peer-review under responsibility of KES International.

*Keywords:* VANET networks; channel modeling; vehicle to vehicle communication; large-scale fading; small-scale fading;

---

### 1. Introduction

With the rapid growth of networked devices for industrial environments and the commercialization of high-speed, short-range wireless interfaces provides the opportunity to deploy a range of useful and practical inter-vehicular communication applications [1] - [2].

---

\* Corresponding author. Tel.: 1 (418) 545 - 5011.

Department of Applied Sciences, University of Quebec in Chicoutimi (UQAC),  
Chicoutimi, G7H 2B1, Québec, Canada

*E-mail address:* [achehri@uqac.ca](mailto:achehri@uqac.ca)

In the last couple of years, communication between vehicles, often referred to as vehicular ad hoc networks (VANETs), have attracted the interest of many researchers across the world [3] - [4].

The harsh physical environment and distinct topology make mining dangerous act as a barrier or restriction to the very techniques and technologies that could improve safety and productivity [5] - [7].

The uses of the vehicle to vehicle communication in the mining industry are expected to open significant opportunities for collecting and exchanging data, localization, collision warning and up-to-date traffic in order improve the safety and productivity of workers in underground mines galleries.

However, many important aspects of vehicular ad hoc networks have not yet been thoroughly investigated in this kind of environments. Successful wireless communications require an understanding of the radio frequency (RF) propagation channel in mine tunnels [8].

Environments in mining environments are particularly harsh with the presence of severe reflection and scattering. As a result, radio signals within such environments suffer from both amplitude and delay distortion. The delay distortion introduces inter-symbol interference and puts a limit on the maximum data rate. Therefore, accurate representation and understanding of the wireless channel will inevitably help to improve the performance of the VANET networks [9] - [10].

Despite many measurement campaigns were conducted up to now, there are still omitted environments and frequency bands, which require to be intensively investigated. Also, the existing models for VANET channel characterization and propagation modeling have been examined in city streets and highways [11] - [12].

This work differs with the papers (i.e. [9], [12]). The underground mines gallery are different from the road tunnels because the rough walls are higher than that in a tunnel with smooth walls (please see Fig 1). The environment in underground mines consists mainly of very rough walls, and the floor is not very flat. It is along these

In this work, we present an analysis of large and small-scale channel modeling for VANET communication in underground mines. Furthermore, we examined various scenarios and possibilities for using VANET communication in underground tunnels.

The contribution of this paper is fivefold. First of all, the channel measurements in the underground environments are performed and analyzed at 5.9 GHz, which have not been detailed in previous works [13] - [14]. Second, the omnidirectional path loss models are characterized based on “well-known” free-space reference distance model.

In addition, a comprehensive parameter table of path loss parameters is given. Large-scale modeling is an important characteristic for link budget calculation and VANET system design. Third, the shadow fading is analyzed. The fourth part of the contribution is to investigate the different distribution models in terms of the average received power. Finally, the statistical analysis of the RMS delay spread for underground mines galleries scenarios is described using measurement datasets.

The paper is organized as follows: in the next section, we give details about the environment and methodology. The measurement setup is described in Section 3. The results and analysis of large-scale models are presented in Section 4. The small-scale modeling is provided in Section 5. Finally; conclusions are drawn in Section 6.

## 2. Environment and Methodology

This work has been carried out by the Underground Communications Research Laboratory (LRTCS). Propagation measurements were performed at 5.8 GHz in an experimental underground mine in Val-d’Or, Canada. In the mining environment, due to the electromagnetic waves propagation complexity, one of the major problems is the radio coverage definition [15].

A complicated way to characterize a channel is to acquire parameters of a deterministic model (i.e., Ray-Tracing simulations). However, this approach turned out to be very complex and limited in capturing the nature of propagation in a confined gallery with rough surfaces [16].

An interesting approach is to make an intensive measurement campaign to extract an empirical model of channel characteristics in underground mines.

### 2.1. Underground Mining Environment

Measurements were conducted in a real underground mine. This former gold mine is located approximately 530 kilometers north-west of Montreal and is now managed by MMSL CANMET (Mining and Mineral Sciences Laboratories-Canadian Center for Minerals and Energy Technology) in which, in field tests and trials can be

performed.

The gallery is located at a 70 m deep underground level. It stretches over a length about 140 m with dimensions that vary between 2.5 m and 3 m in width and a height of nearly 3m. Photography of the underground gallery is shown in Fig.1.



Fig.1. Photography of the mine gallery.

The environment consists mainly of very rough walls, and the floor is not very flat. It is along these walls that cables and pipes are stretched (near the ceiling). The temperature is stable at  $6 - 7^{\circ} \text{C}$ , with a humidity level of nearly 100% throughout the year and water dripping everywhere; there are some areas of water puddles with different dimensions of up to several meters in length. Other elements such as ventilation and screens that cover the ceiling of the gallery contribute to the multipath phenomenon.

Fig.2 shows the 70 m underground level plan with all galleries available. The site chosen allows a direct line of sight (LOS) communication. This part of the gallery is a well-controlled environment providing reliable results. This site is far from any industrial activity.

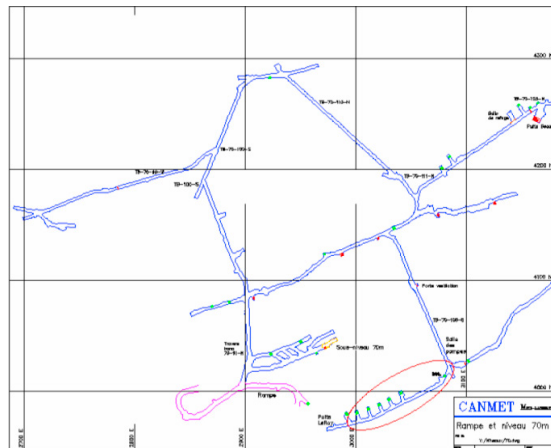


Fig.2. Map of level 70 m and the site chosen for the measurement campaign.

### 3. Measurement Setup

Before starting the measurements, the system was calibrated. Moreover, all the measurement system parameters like transmitting power, frequency bandwidth, and frequency resolution were well configured. The analyses were conducted in the frequency domain in which the channel impulse responses (CIRs) were measured and recorded.

The goal of the measurements was to investigate the small and the large-scale variations of the channel. Large-scale variations are due to high antenna separations changes, one meter for instance, where small-scale variations indicate changes in channel behavior when the antenna's of the receiver move by a corresponding, a fraction of wavelength distance.

To compute the large and small-scale parameters, we used a vector network analyzer VNA (Agilent E8363B). The magnitude and phase of  $S_{21}$  scattering parameter are acquired at the different stepped point of frequency bandwidth. The VNA recorded 401 complex points in the frequency range from 5.85 to 5.925 GHz. The power level transmitted by the VNA was set to -20 dBm to comply with the maximum input power of the RF-Lambda LNA (RLNA01M10G). It covers a frequency range from 5.85 to 5.925 GHz, and the noise figure is stable along the frequency range. The gain of the power amplifier is equal to 30 dB.

The two ports of the VNA are connected to the transmitter and receiver (RD2458-5). The transmitting antenna is connected to port number 1 of the VNA While the receiving antenna was connected to port 2. The height of both antennas is 2m above ground.

The transmitting antenna remained in a fixed position while the receiving antenna was placed in a vehicle that moved along the gallery while taking measurements corresponding to the different speeds of the vehicle (Fig.3).

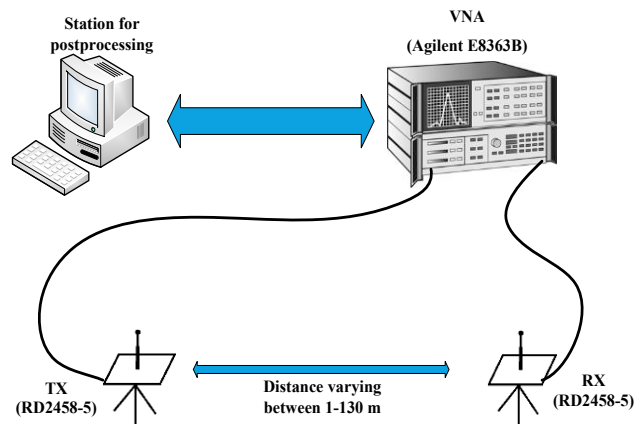


Fig.3. Channel measurement setup for the first scenario.

In the second scenario, to study the effect of speed on received signal power. We used a spectrum analyzer (Anritsu MS2687B) and two similar omnidirectional antennas with directional radiation patterns identical to those of the former scenario. An Anritsu MG3700A signal generator generated a single narrowband sinusoid signal whose carrier frequency set to 5.9 GHz. An antenna fixed on the wall emits this signal. On the other side, a receiving antenna linked to the spectrum analyzer (Anritsu MS2687B) was placed in a vehicle that moved along the gallery while taking measurements corresponding to the different speeds of the vehicle (Fig. 4).

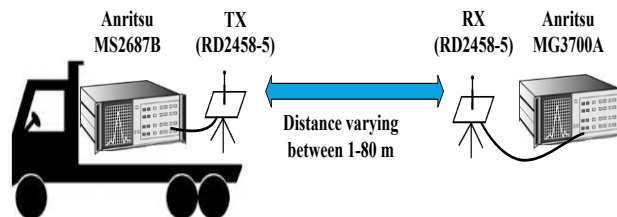


Fig. 4. The measurement system for the second scenario.

## 4. Large-scale Modeling

### 4.1. Frequency response

The frequency response  $H(f)$  is defined by the following relation:

$$H(f) = |H(f)| \cdot e^{j\theta(f)} \quad (1)$$

Figure 5 shows an example of a channel frequency response for a distance separation Tx-Rx of 8 meters in a LOS situation. The figure illustrates the amplitude, in dB, and the phase, in degrees, of the complex frequency response.

The channel is considered a linear time-varying system. The channel impulse response  $h(t)$  can be described as follows:

$$h(\tau; t) = \sum_{k=0}^{N-1} a_k \delta(t - t_k) e^{j\theta_k} \quad (2)$$

where  $N$  is the number of multiple paths.  $a_k$ ,  $\theta_k$ , and  $t_k$  are respectively the random amplitude, the phase, and time of arrival of the  $k$ th path, and  $\delta$  is the delta function.

The impulse response  $h(\tau, t)$  was derived from the frequency response by making an inverse discrete Fourier transform of  $H(f, t)$ .

$$h(\tau; t) = \frac{1}{N} \sum_{k=0}^{N-1} H(f_k, t) e^{j2\pi \frac{\tau k}{N}} \quad (3)$$

The impulse responses have a temporal resolution of 13.3 ns, which is the inverse of the bandwidth of 75 MHz.

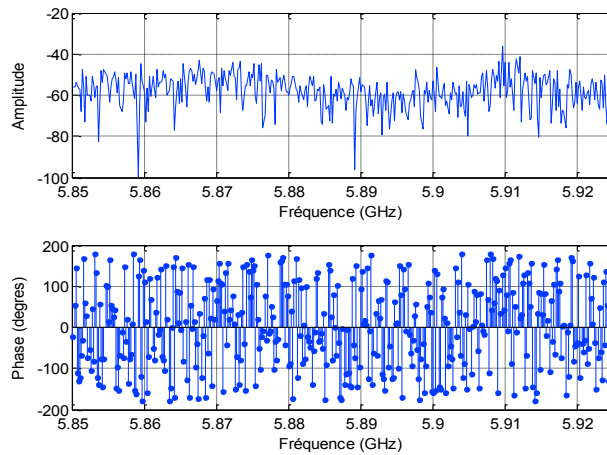


Fig. 5. Amplitude and phase of the frequency response.

### 4.2. Path loss

A large-scale measurement is performed to evaluate the propagation distance-power profiles in the underground mine environment. The path loss is a significant parameter which can be applied to describe the large-scale effects of the propagation channel.

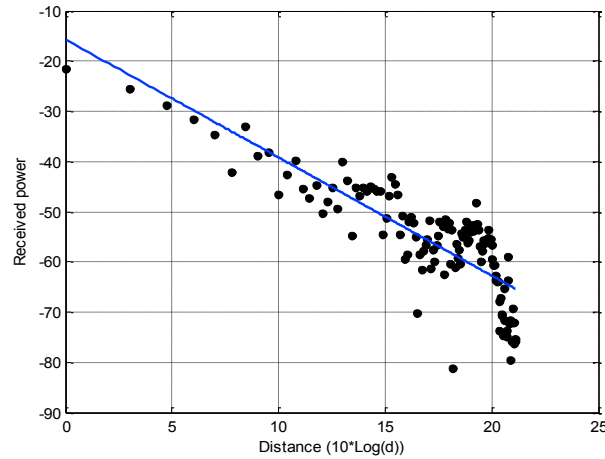


Fig. 6. The average received power vs. the distance Tx-Rx.

Fig. 6 represents the path loss as a function of distance. Equation (4) was used to compute the mean path loss referenced to a distance  $d_0$  for each spatially averaged power impulse responses [15].

$$PL(d) = PL_0 + 10.n.\log_{10}\left(\frac{d}{d_0}\right) + S(d), \quad d > d_0 \quad (1)$$

The parameter  $d_0$  is the reference distance (in our case  $d_0=1$  meter),  $PL_0$  is the reference point path loss,  $n$  is the path loss exponent, and  $S$  is the shadowing fading parameter that varies randomly from one location to another. In this paper, the average power for each measurement is calculated by averaging the power over all sample points of the measured frequency response. By using linear regression analysis, the minimum mean square error (MMSE) line is calculated for the average measured power (dB) over the logarithm of the distance for each experiment. The slope of the regression line gives the experimental value of  $n$ .

The linear regression analysis gives the path loss exponent  $n$ , the path loss at the reference distance  $PL_0$  and the correlation coefficient for all measurements.

Tab. 1 Path loss parameters for different scenarios.

	0 m/s	1 m/s	2 m/s	4 m/s	5 m/s
$n$	2.0479	2.1624	2.1890	2.4146	2.4826
$PL_0$	-15.7231	-22.3078	-23.0419	-18.7879	-21.2040
Correlation coefficient	-0.83354	-0.87628	-0.87981	-0.89924	-0.91876

Table 1 shows that the path loss exponent varies between 2.16–2.41, near to those obtained in the literature for underground mines environments [15] - [19], where they found that the path loss exponent is in the range 1.59 – 4.

### 4.3. Shadow Fading

Due to variations in the surrounding environments, the power loss PL observed at any given location will deviate from its average value. This phenomenon is called shadow fading. The shadow fading parameter is provided by the term  $S$  that varies randomly from one location to another.

The cumulative distribution function (CDF) of the deviation between the fitted and measured data is plotted

versus the normal distribution with parameters  $\sigma$  and  $\mu$  in dB (Fig. 7). These curves show that the shadow fading is lognormally distributed.

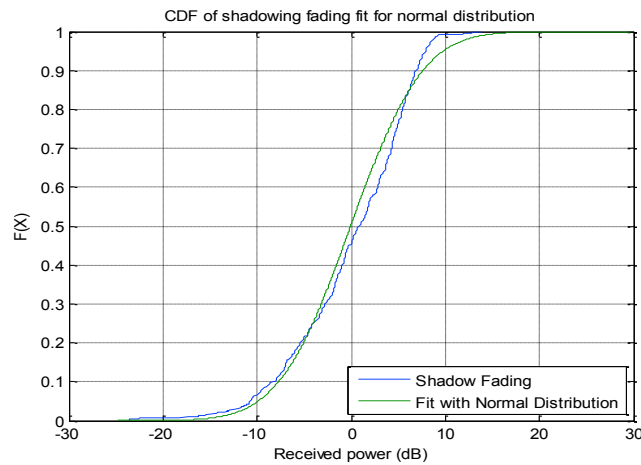


Fig. 7. The CDF of the shadow fading fit for with normal distribution.

The statistical analysis of the parameters  $S$  shows that the shadow fading follows a Normal distribution with mean 0 dB and different standard deviations  $\sigma$  varying from 3.8 – 6 dB depending on the speed as shown in table 2.

Table 2. The variance of the shadow fading fit with the normal distribution.

	0 m/s	1 m/s	2 m/s	4 m/s	5 m/s
variance $\sigma$	6	5	5.2	4.8	3.8

## 5. Small-scale Modeling

### 5.1. Received Average Power

In VANET wireless communication channels, the signal is transmitted and then undergoes direct reflection, transmission, scattering, and diffraction. Hence, the signal arriving at the receiver is the superposition of the various multipath components.

The cumulative distribution functions (CDF) of the measured received power are shown in Figure 8. To determine the best distribution that fits with the experimental results, we chose the Kolmogorov-Smirnov (KS test) to compare the obtained results with some well-known functions using the following formula:

$$D = \max|f_T - f_S| \quad (5)$$

where  $f_T$  is the theoretical CDF and  $f_S$  is the experimental CDF. The distribution having the smallest distance is considered to be the function that best represents the experimental data.

Table.3. Statistics of the received average power.

	0 m/s	1 m/s	2 m/s	4 m/s	5 m/s
Nakagami	m=5.3	m=5.3	m=5.5	m =5.5	m=5.5
	$\Omega=1.1$	$\Omega=1.1$	$\Omega=1.1$	$\Omega=1.1$	$\Omega=1.1$
D	0.122	0.125	0.126	0.103	0.101
Log-normal	$\sigma=0.2$	$\sigma=0.1$	$\sigma=0.2$	$\sigma=0.2$	$\sigma=0.2$
D	0.088	0.114	0.101	0.078	0.072
Weibull	k = 1.1	k = 1.1	k = 1.1	k = 1.1	k = 1.1
	$\lambda = 4.1$	$\lambda = 4.9$	$\lambda = 5$	$\lambda = 5$	$\lambda = 5$
D	0.134	0.133	0.126	0.105	0.103

As shown in figure 7 and highlighted in table 3, the Kolmogorov-Smirnov test concludes that the Lognormal distribution is the best fit for the measured average power.

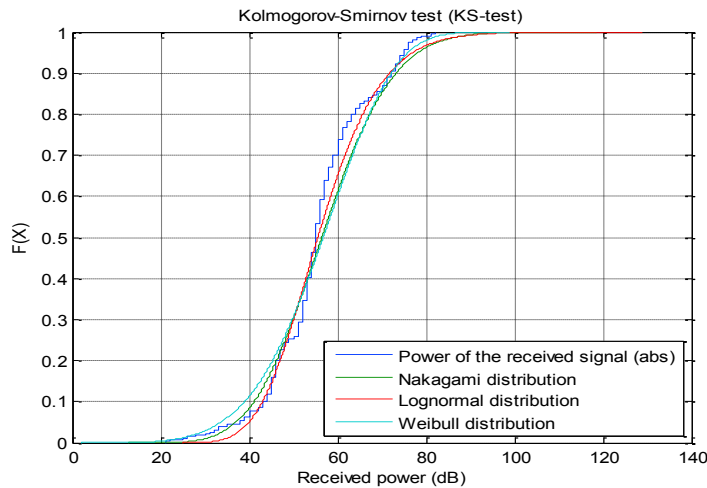


Fig.8. Comparative curve between the different distributions and experimental results.

### 5.2. Delay spread

The mean excess delay and root-mean-square (RMS) delay are two essential parameters used to characterize the temporal dispersive properties of multipath channels. The mean excess delay  $\bar{\tau}$  is defined as the first moment of the power delay profile (PDP):

$$\bar{\tau} = \frac{\sum_k p(t_k)t_k}{\sum_k p(t_k)} \tag{7}$$

where  $p(t_k)$  and  $t_k$  are the power and the delay of the  $k^{th}$  path, respectively.

The underground mines are considered a very rich multipath environment because of the presence of many reflectors, the very rough wall, and the complexity of the topology [15]-[19]. The parameter that allows us to measure multipath richness is called the RMS delay spread  $\tau_{RMS}$ . This parameter determines the frequency selectivity of the channel and the maximum data rate for the multiuser systems. The formula used to calculate the RMS delay spread is given by:



$$\tau_{RMS} = \sqrt{\tau^2 - \bar{\tau}^2} \quad (6)$$

Where  $\bar{\tau}$  is the mean excess delay given in Eq. (7) and  $\bar{\tau}^2$  is the second moment of the PDP.

The delay dispersion was characterized by cumulative distribution functions of the  $\tau_{RMS}$  delay spreads, the values for CDF=0.9 varied from 15 to 85 ns in different scenarios while the mean excess delay varied from 18 ns to 110 ns.

## 6. Conclusion

This paper presented the first study of channel modelling for VANET communication in underground mines at 5.9 GHz. The primary purpose of this study is to measure and characterize large-scale, small-scale fading and extract some time channel parameters such as RMS delay spread for a realistic underground propagation environment.

The path loss models show a large variety of path loss exponent, values of similar setups varied between 2.04–2.48 so that the highest values were found with the high-speed velocity. The variability of implies that reliable operation range of high capacity VANET networks at 5.9 GHz. We have also seen that the variation of the received signal power follows a Lognormal distribution. Furthermore, for most scenarios (90% of the cases), values of  $\tau_{RMS}$  are less than 85 ns. The results presented herein (with other works) could be used in the design and evaluation of a VANET performance in underground mining environments.

The results presented herein (with other works) could be used in the design and evaluation of V2V and V2I networks in underground mining environments. Future work includes analysis to develop a model for the LOS-to-NLOS transitions to enable a complete “two-state” fading V2V channel model for underground mines and the incorporation of time-varying properties of a multiple-input multiple- output (MIMO) vehicle-to-vehicle propagation channel. Future work will consist in investigating channel dynamics and spatial correlations, and in comparing our results with the IEEE 802.11p model.

Future work will consist in investigating channel dynamics and spatial correlations, and in comparing these results with other models.

## References

- [1] Ankita, Khapekar and Rajesh, Shekocar (2014) "Vehicular Communication - A Survey", *IET Networks*, **3** (3): 204-217.
- [2] Maryam, Alotaibi and Mouftah, Hussein (2017) "Relay selection for heterogeneous transmission powers in VANETs", *IEEE Access*, **5**: 4870-4886.
- [3] MacHardy, Zachary, Khan, Ashiq, Obana, Kazuaki, and Iwashina, Shigeru (2018) "V2X Access Technologies: Regulation Research and Remaining Challenges", *IEEE Communications Surveys & Tutorials*, **20** (3): 1858-1877.
- [4] Boualouache, Abdelwahab, Senouci, Sidi-Mohammed, and Moussaoui, Samira (2018), "A Survey on Pseudonym Changing Strategies for Vehicular Ad-Hoc Networks", *IEEE Communications Surveys & Tutorials*, **20** (1): 770-790.
- [5] Chehri, Abdellah, Fortier, Paul, and Tardif, Pierre-Martin (2008) "An investigation of UWB-based wireless networks in industrial automation", *Int. J. Comput. Sci. Network Security*, **8** (2): 179-188.
- [6] Chehri, Abdellah, Farjow, Wissam, Mouftah, Hussein, and Fernando, Xavier (2011) "Design of Wireless Sensor Network for Mine Safety Monitoring," *IEEE Canadian Conference on Electrical and Computer Engineering* : 1532-1535.
- [7] Chehri, Abdellah, Fortier, Paul, and Tardif, Pierre-Martin (2007) "Security Monitoring Using Wireless Sensor Networks," *IEEE Commun. Networks and Services Research*: 13-17.
- [8] Chehri, Abdellah, Fortier, Paul, and Tardif, Pierre-Martin (2008) "Large-scale fading and time dispersion parameters of UWB channel in underground mines", *Int. J. Antennas Propag.* Article ID 806326.
- [9] Karedal, Johan, Czink, Nicolai, Paier, Alexander, Tufvesson Fredrik, and Molisch Andreas F. (2011) "Path Loss Modeling for Vehicle-to-Vehicle Communications", *IEEE Transactions on Vehicular Technology*, **60** (1): pp.323-328.
- [10] Cheng Li, Henty Benjamin E, Stancil Daniel D, Bai Fan, and Mudalige Priyantha (2007) "Mobile Vehicle-to-Vehicle Narrow-Band Channel Measurement and Characterization of the 5.9 GHz Dedicated Short-Range Communication (DSRC) Frequency Band", *IEEE Journal on Selected Areas in Communications*, **25** (8): 1501-1516.
- [11] Abbas, Taimoor, Tufvesson, Sjoberg katrin, and Fredrik Karedal, Johan (2012) "Shadow Fading Model for Vehicle-to-Vehicle Network Simulators", COST IC1004 5th Management Committee and Scientific Meeting, Bristol, UK: 1-11.
- [12] Kunisch Jürgen, and Pamp Jörg (2008) "Wideband Car-to-Car Radio Channel Measurements and Model at 5.9 GHz," *Vehicular Technology Conference, IEEE 68th VTC 2008-Fall*:1-5.
- [13] Bernado, Laura, Roma, Anna, Paier Alexander, and Zemen Thomas (2011) "In-Tunnel Vehicular Radio Channel Characterization", *IEEE 73rd Vehicular Technology Conference (VTC Spring)*:1-5.

- [14] Lored, Susana, del Castillo, Adrian, Fernández, Herman, and Rodrigo-Peñarrocha, Vicent (2017) "Small-Scale Fading Analysis of the Vehicular-to-Vehicular Channel inside Tunnels," *Wireless Communications and Mobile Computing*, Article ID 1987437.
- [15] Chehri, Abdellah, Fortier Paul, and Tardif, Pierre-Martin (2012) "Characterization of the ultra-wideband channel in confined environments with diffracting rough surfaces", *Wireless Pers. Communication*, **62** (4): 859-877.
- [16] Chehri, Abdellah, Fortier, Paul, Aniss, Hasnaa, and Tardif, Pierre-Martin (2006) "UWB spatial fading and small-scale characterization in underground mines", *IEEE Proc. 23rd Biennial Symp. Commun.*: 213-218.
- [17] Benzakour, Ahmed, Affes, Sofiène, Despins, Charles, and Tardif, Pierre-Martin (2004) "Wideband measurements of channel characteristics at 2.4 and 5.8 GHz in underground mining environments", *IEEE VTC 2004-Fall*: 3595-3599
- [18] Nerguzian, Chahé, Despins, Charles, Affes, Sofiène and Djadel, Mourad (2005) "Radio Channel Characteritization of an Underground Mine at 2.4 GHz", *IEEE Transactions on Wireless Communications*, **4** (5): 2441-2453.
- [19] Boutin, Mathieu, Affes, Sofiène, Despins, Charles, and Denidni, Tayeb (2005) "Statistical Modelling of a Radio Propagation Channel in an Underground Mine at 2.4 and 5.8 GHz", *IEEE 61st Vehicular Technology Conference VTC-Spring*: 78-81.